PHYSICAL REVIEW B VOLUME 49, NUMBER 11 15 MARCH 1994-I

Surface and bulk modulation in photoreflectance from undoped GaAs

Michael Sydor, James R. Engholm,* Daniel A. Dale,* and T. J. Fergestad
Department of Physics, University of Minnesota, Duluth, Minnesota 55812
(Received 2 August 1993; revised manuscript received 22 October 1993)

Plasma discharge is used to alter the surface potential in undoped GaAs. The results determine the origin and the magnitude of photomodulation in photoreflectance from undoped GaAs. We examine photoreflectance for 30–70-kV/cm surface electric fields in undoped GaAs grown on heavily doped n- or p-type GaAs underlayers, UN^+ and UP^+ samples, respectively. Photoreflectance for 2–500-μW/cm^2 laser modulation intensity was analyzed using separate electro-optic functions to determine the magnitude of the built-in electric field in the dark and the laser illuminated samples. Before plasma discharge, photomodulation of the built-in electric field in UP^+ samples was about three times that in UN^+ samples at 0.2 mW/cm^2. The large modulation in UP^+ samples appears to have come from surface modulation effects, possibly from poor pinning of the surface Fermi energy. A hydrogen plasma discharge lasting 4 s produced long term effects in UP^+ samples. It increased the magnitude of the electric field in UP^+ samples from $\sim$40 kV/cm to $\sim$60 kV/cm, at 0.2 mW/cm^2. The discharge more than doubled the amplitude of UP^+ photoreflectance signal and increased the number of Franz-Keldysh oscillations. After discharge, the photomodulation voltage for UP^+ samples was reduced from 0.32 to 0.14 V at 0.2 mW/cm^2, and became comparable with bulk photovoltage from (p-i-n) structures and UN^+ structures.

INTRODUCTION

In photoreflectance (PR), we measure the changes in reflectance produced by modulating a sample's built-in electric field $\mathcal{E}$ with a chopped laser beam.[1,2] The effect of photomodulation is very similar to the modulation of $\mathcal{E}$ by an external ac electric field.[3,4] However, the mechanism and the origin of photomodulation can be quite complex because it can come from depletion-layer photocurrents and surface charge fluctuations.[5–7] We examine here the magnitude and the origin of photomodulation of $\mathcal{E}$ in undoped GaAs.

Undoped GaAs has a band gap of 1.424 eV, and has its surface Fermi energy pinned $\sim$0.75 eV below the conduction band.[8] The pinning of surface Fermi potential (V_F) gives rise to conduction-band bending and a built-in $\mathcal{E}$ whose magnitude and direction depend on the sample structure and sample illumination.[9–12] The pinning of V_F for a free GaAs surface comes from adsorbant-vacancy states,[8,13] whose distribution and properties with illumination are not fully understood and are the subject of recent investigations.[9–12] For instance, it is not known whether surface charge trapping can affect the pinning of V_F. Photogenerated electrons or holes can accumulate at the surface depending on the direction of $\mathcal{E}$. The accumulated carriers can reduce $\mathcal{E}$ because of charge separation, or by affecting the occupation probability of the surface states which in turn affect V_F. We estimate the magnitude of photomodulation due to depletion-layer photocurrents versus the possible surface effects by comparing PR for two complementary structures, UP^+ and UN^+.[9] The structures should have comparable but reversed $\mathcal{E}$. The built-in field is uniform and is confined almost exclusively to the undoped layer of GaAs.[9] Thus, by measuring PR and calculating $\mathcal{E}$ and $\Delta\mathcal{E}$ we can estimate the illuminated surface potential and the magnitude of total photomodulation voltage V_s. Since $|\mathcal{E}|$ is generally presumed comparable for both structures, the magnitude of photocurrents in the undoped layer of GaAs should also be comparable;[12] after all, the conductivity of undoped GaAs is the same in UP^+ and UN^+ structures, and both structures are assumed to have equivalent surface-state properties and V_F pinned at $\sim$0.75 V independent of illumination.[6,9,11] We will see that the assumption of equivalent surface-state properties and V_F is suspect because the structures display larger differences in PR and V_s at equivalent intensities.[6,9–11]

The UP^+ structures show roughly two thirds the value of $\mathcal{E}$ in comparison with the UN^+ samples at the same illumination.[10] The relatively low fields in UP^+ have been attributed to a logarithmic dependence of photovoltage on the sample illumination intensity.[6] However, the differences in the magnitude of V_s for UN^+ and UP^+ structures remain unresolved.

In this study, we calculate $\mathcal{E}$ and $\Delta\mathcal{E}$ independent of the origin of PR modulation. We simulate PR with two electro-optic functions that account for the dark and the laser-illuminated magnitudes of $\mathcal{E}$. Subsequently, we expose the samples to a plasma discharge to alter V_F and estimate the fraction of V_s for a free GaAs surface that can be attributed to a depletion-layer photovoltage and surface photomodulation.

EXPERIMENT

A schematic of PR apparatus is shown in Fig. 1. The changes in reflectance between the laser-illuminated and the dark conditions are detected with a standard ac lock-

0163-1829/94/49(11)/7306(7)/$06.00 ©1994 The American Physical Society

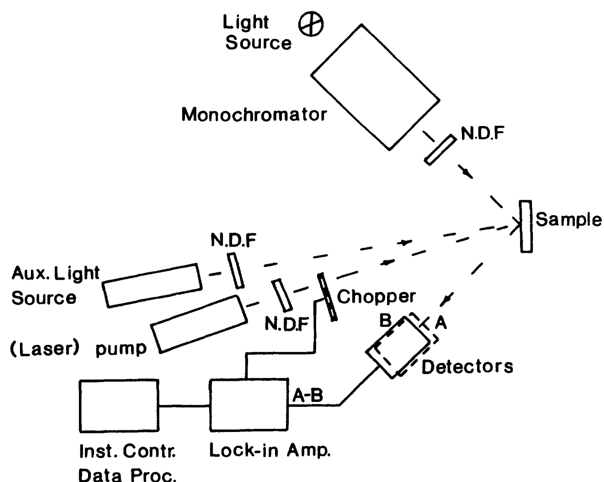

FIG. 1. Schematic of photoreflectance apparatus. Detector B lies out of the plane of incidence and responds to the scattered light and room-temperature photoluminescence that are subtracted out in the A-B mode on the lock-in amplifier.

in technique. The dark condition refers to a 0.3 μW/cm^2 probe beam illumination. An additional detector B in Fig. 1 lies out of the plane of incidence. The secondary detector responds to scattered light and to room-temperature photoluminescence. Using the two detectors operating in a subtraction mode we eliminate the scattered light, the PL, and much of the cable pick-up noise.

Measurements were made on six (three each) 100-nm-thick samples of undoped GaAs grown by molecular beam epitaxy (MBE) on top of 100-nm heavily doped p- or n-type GaAs underlayers. For UN^+ samples we had undoped 100-nm GaAs layer grown by MBE on a 100-nm Si-doped (6×10^{18} cm^{-3}) GaAs underlayer, backed by a 1-μm undoped GaAs buffer and semi-insulating GaAs substrate. For the UP^+ samples we had a 100-nm undoped GaAs layer grown on a 100-nm Be-doped (10^{19}/cm^3) underlayer backed by a 1-μm undoped GaAs buffer and semi-insulating GaAs substrate. The underlayers pin the Fermi level in the valence band or the conduction band, depending on Be or Si doping.[9,10] The sample configurations produce $\sim$70 kV/cm uniform electric field with opposing directions in UP^+ and UN^+ structure.[6,9–12] We examined the uniformity of $\mathcal{E}$ as a function of laser penetration depth at different wavelengths, and used an additional steady illumination source to provide an optical bias when we measured $\mathcal{E}$ independent of the chopping frequency.[14] The wavelength of the pump and the steady-bias light source ranged from 380 to 700 nm. The steady illumination decreases the magnitude of $\mathcal{E}$.

To examine the effect of plasma discharge on V_F, we performed PR measurements in air, vacuum, hydrogen gas at atmospheric pressure, and hydrogen at vacuum. Subsequently, we created an *in situ* 4-s discharge at 700 V in H_2 at $\sim10^{-2}$ Torr pressure. PR measurements followed within a few minutes after the discharge, several times thereafter, and again at atmospheric pressure and days afterward to determine time-dependent effects. The procedure was repeated on a duplicate set of samples using an Argon discharge. All measurements were performed at room temperature.

Calculations of $\mathcal{E}$ and $\Delta\mathcal{E}$ were based on PR theory.[3] For the UN^+ samples, we usually observed 14–20 well defined Franz-Keldysh oscillations (FKO).[10] The FKO had pronounced beatlike envelopes (see Fig. 2) whose reproduction by theoretical means lent credence to the analytical methods. We tested the accuracy of the calculated electric fields by using duplicate PR measurements and by examining the variance in $\mathcal{E}$ for equivalent samples.

Generally, V_s reduces the magnitude of $\mathcal{E}$ for either direction of $\mathcal{E}$.[3,6,11] We take $V_s=(|\Delta\mathcal{E}|\times d)$ V, independent of the sign of $\mathcal{E}$ and the origin of modulation. d is the thickness of the undoped layer of GaAs. We neglect the depletion region in the highly doped underlayers, assume a uniform $\mathcal{E}$, and neglect the 0.3-μW/cm^2 probe-beam intensity. Thus, $(\mathcal{E}_{\rm dark}\times d)$ V should approach $V_F\sim0.75$ V for the UN^+ samples, and $(1.424-V_F)$ V

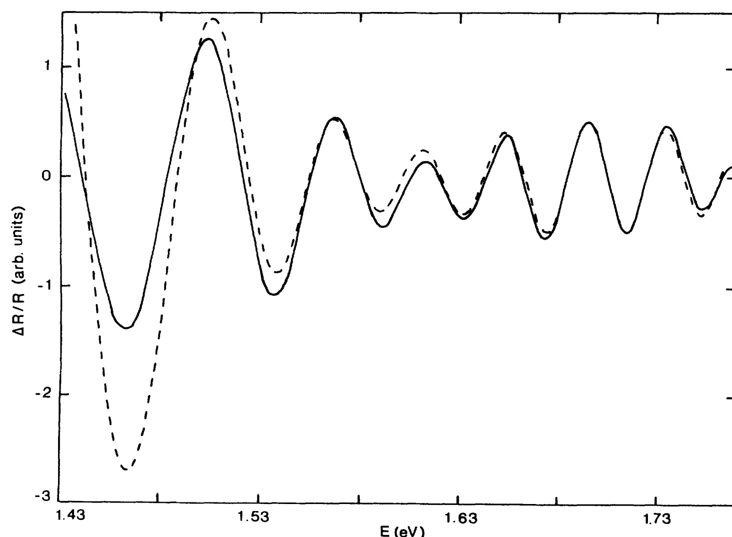

FIG. 2. Photoreflectance spectrum and its single-function theoretical fit (broken line) to the UN^+ sample. The fit yields an electric field $\mathcal{E}=70.3$ kV/cm at 0.3 mW/cm^2 441.6-nm intensity, and a band gap $E_g=1.422$ eV.

for the UP^+ samples.[9] For the sake of comparison we also define $V_b = (\mathcal{E}_{\rm FKO} \times d)$ V, and note that in our case V_s is not equal to a fixed $V_F - V_b$.[11,12]

DETAILS OF NUMERICAL CALCULATIONS

In the calculation of $\mathcal{E}$ we relied on the theory and the results presented in Refs. 3 and 15–17. The assumptions and the general background on modulated reflectance theory can be found in the second of the Aspnes articles cited in Ref. 3. For modulation from *flatband,* the general solution valid for the high-field condition yields a typical oscillatory behavior for modulated reflectance $\Delta R/R$ in terms of the electro-optic functions,[16,17]

$$\Delta R/R = \alpha_{\rm lh} G[(E-E_g)/\hbar\theta_{\rm lh}] + \alpha_{\rm hh} G[(E-E_g)/\hbar\theta_{\rm hh}] , \quad (1)$$

where $G(x)$ is given by the Airy functions and their derivatives according to

$$G(x) = {\rm Ai}'(x){\rm Bi}'(x) - x\,{\rm Ai}(x){\rm Bi}(x) ,$$
$$(\hbar\theta_{ih})^3 = e^2\hbar^2\mathcal{E}^2/2\mu_{ih} , \quad i = l \text{ or } h , \quad (2)$$

E is the probe-beam energy, E_g is the band-gap energy, $\mathcal{E}$ is the uniform electric field, and $\mu_{\rm lh}$ and $\mu_{\rm hh}$ are the reduced effective masses for the light and the heavy holes, respectively. For flatband modulation, the band edge and the electric field at the sample surface can be found by fitting the PR trace with solution (1). When the modulation from the flatband condition is not satisfied, Shen[18] shows that the first derivative of the electro-optic functions with respect to the field should be included in the theoretical fits in Eq. (1). We did so, depending on the total illumination level. Cursory examination of the oscillatory nature of the electro-optic function quickly shows that the derivatives of the electro-optic functions produce little change in the periods of FKO. However, the derivatives underestimate the amplitude of PR near the band-gap energies. Thus, we determined that the modulation of $\mathcal{E}$ for our samples was large even at several μW/cm^2 laser intensity. To obtain a close fit to the data over the entire range of the PR spectrum we had to fit the PR with a subtraction of separate electro-optic functions for the illuminated and the dark fields, allowing for the finite nature of PR modulations that we observed experimentally.

The numerical fit of the superposition of electro-optic functions to the data was accomplished using a modification of the Marquardt gradient-expansion algorithm,[19] with the electric field, energy gap, and the light- and heavy-hole coefficients $\alpha_{\rm lh}$ and $\alpha_{\rm hh}$, used as the fitting parameters. The modifications were necessary because of the shape of the χ^2-parameter space. The hole coefficients have a well defined joint minimum in χ^2 space for any given band-gap and field values, while the gap and field parameters have a very broad and shallow joint minimum which the unmodified algorithm had trouble locating. The modification to the algorithm consisted essentially of forcing the step size in the electric-field parameter to have a definite minimum value until the fit became sufficiently good to allow the program to have free control over it. The approach to the minimum in χ^2 space was made from both higher and lower field values in order to verify the minimum.

$(\hbar\theta_{ih})^3$ in the theory due to Aspnes and co-workers[16] is defined only to within the ratio of $\mathcal{E}^2/\mu_{ih}$. Thus, any study of the effective masses is ambiguous with respect to the field values when the fields are unknown. For this reason and for direct comparison with published results, we used the accepted values of the reduced electron masses.[9]

A quick and most commonly used method for determining the band-gap energy and the electric field was performed according to its treatment due to Bhattacharya *et al.*[20] and Bottka *et al.*,[21] who used an approximate form of Eq. (1),[16]

$$\Delta R/R \cong \cos\{(\tfrac{2}{3})[(E-E_g)/\hbar\Omega]^{3/2} + \pi(d-1)/4\} , \quad (3)$$

to obtain a graphical determination of $\mathcal{E}$. In Eq. (3), d is the dimensionality of the critical point. GaAs has a direct band-to-band transition, so we can take $d = 3$. If we neglect the amplitude factor in Eq. (3), the position of the FKO extrema can be approximated by

$$E_j = \hbar\Omega(F_j) + E_g , \quad j = 1,2\ldots, \quad (4a)$$

$$F_j = [3\pi(j-\tfrac{1}{2})/2]^{2/3} \quad (4b)$$

$\hbar\Omega$ is a characteristic energy associated with the critical point and is related to the electric field $\mathcal{E}$ by

$$\hbar\Omega = (e^2\mathcal{E}^2\hbar^2/8\mu)^{1/3} , \quad (5)$$

where μ is the interband reduced mass.

As indicated by Eq. (4), a plot of E_j versus F_j is a straight line with slope $\hbar\Omega$, and intercept E_g. The plot uses successive FKO extrema marked $1,2,\cdots$, following the main PR peak at the band edge.[20] The intercept E_g determined from PR in this manner usually falls close to the band-gap energy. For electroreflectance data, the fields obtained from Eq. (4) are generally close to the measured fields.[3,16] As a result, the FKO method is frequently taken for granted in the analysis of PR data.

RESULTS

Figure 2 shows an example of PR data in the FKO energy region together with a single-function theoretical fit according to Eq. (1). Notice the pronounced beatlike envelope of the FKO oscillations.[9] Single electro-optic functions provided reasonable fits to the data in the FKO region and gave reproducible values for the band-gap energy and the electric fields.

Graphical plots according to Eq. (4), as exemplified in Fig. 3, produced electric fields and band-gap values in fair agreement with the single-electro-optic-function fits. For UN^+ samples, FKO plots produced electric fields $\sim 3\%$ lower than the single-function fits. $\mathcal{E}$ for our UN^+ samples was 73 kV/cm at ~ 10 μW/cm^2 intensity. This value is in good agreement with the $\mathcal{E}$ for UN^+ samples that have infinitely thick doped underlayers.[6,15]

At any given illumination in the 2–500-μW/cm^2 range, UP^+ samples gave a lower $\mathcal{E}$ than the UN^+ samples.

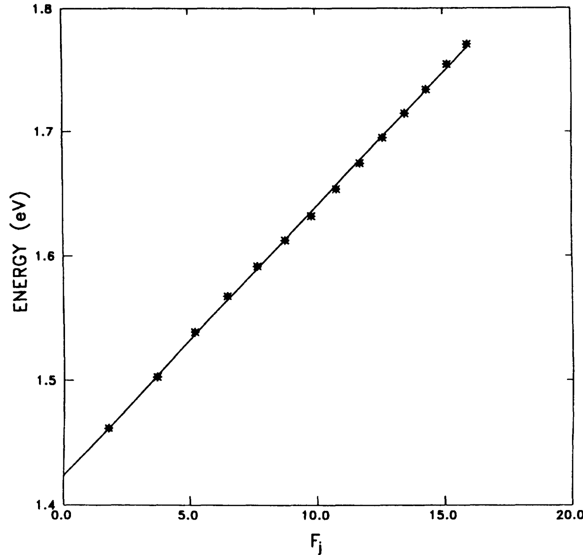

FIG. 3. FKO vs the F_j number for the UN^+ sample before plasma exposure. The plot gives an electric field $\mathcal{E}=69.3$ kV/cm and a band gap $E_g=1.423$ eV for the PR in Fig. 2.

The low fields for UP^+ samples agree with the previously reported results.[9,10] A $\pm 7\%$ scatter observed for $\mathcal{E}$ from the UP^+ samples was due to the relatively short stretches of UP^+ data and the small number of FKO observed for the damped PR from the UP^+ samples. Single electro-optic functions and their derivatives provide a poor fit to PR data in the 1.4–1.5-eV region (see Fig. 2). This region is where we find most of the damped PR signal from the UP^+ samples. Thus, the damped character of UP^+ PR may affect the value of $\mathcal{E}$ calculated from single-function fits and FKO.

The reason for the damped character of the PR spectra from UP^+ samples is difficult to assess. In UN^+ samples the light and heavy holes have a continuum of bound states near the surface from which transitions can take place over a 1.4–1.7-eV range.[22] On the other hand, there are few bound states for the electrons in UP^+ samples. Thus UP^+ PR spectra may be limited to a shorter range.[22] Another reason for the difference in the length of the UN^+ and UP^+ spectra may come from the difference in the magnitude of surface modulation. For instance, we noticed that modulation with polarized laser beams at grazing angles affected the amplitude of FKO relative to the band-edge signal. For single-electro-optic-function fits we found a nearly constant ratio of α_{hh}/α_{lh} of 2.5 for UN^+ samples while the ratio for the UP^+ samples changed with laser wavelength, indicating a dependence in modulation on pump penetration depth. To account for the effect of the magnitude of modulation on the calculation of $\mathcal{E}$, we simply chose to model PR with differences of electro-optic functions that produce better fits over the entire PR spectrum. This procedure does not account specifically for the origin of the beats in UN^+ spectra and damped UP^+ spectra in the manner of more sophisticated models that account for the detailed dependence of reflectance with depth.[16,23,24]

Using different electro-optic functions, we show in Figs. 4 and 5 two-function fits to PR data for UN^+ and UP^+ sample. Unlike the single-electro-optic-function fits, the two-function simulations provide a good fit to PR over the entire 1.42–1.75-eV energy range. Two-function fits yield $\mathcal{E}_{dark}$ of 75 kV/cm and 64 kV/cm for UN^+ and UP^+ samples, respectively. The total potential difference for the dark UN^+ versus dark UP^+ samples is 1.39 V, in fair agreement with the 1.424-eV band-gap energy. FKO-determined fields usually lay between the $\mathcal{E}_{dark}$ and $\mathcal{E}_{illum}$, but the relation changed with intensity. At 0.2 mW/cm^2, UP^+ samples show roughly a factor-of-three higher V_s than the UN^+ samples. We had no definitive explanation for this except by conjecturing that the pinning of V_F could differ in UP^+ and UN^+ samples. To alter V_F we exposed the samples briefly to H_2 plasma. The results based on FKO plots are shown in Fig. 6, and the calculated values of V_s are shown in Fig. 7. The magnitude of V_s for UP^+ samples dropped after plasma discharge from 0.32 to 0.14 V at 0.2 mW/cm^2, compared with 0.12-V modulation in UN^+ and the plasma etched

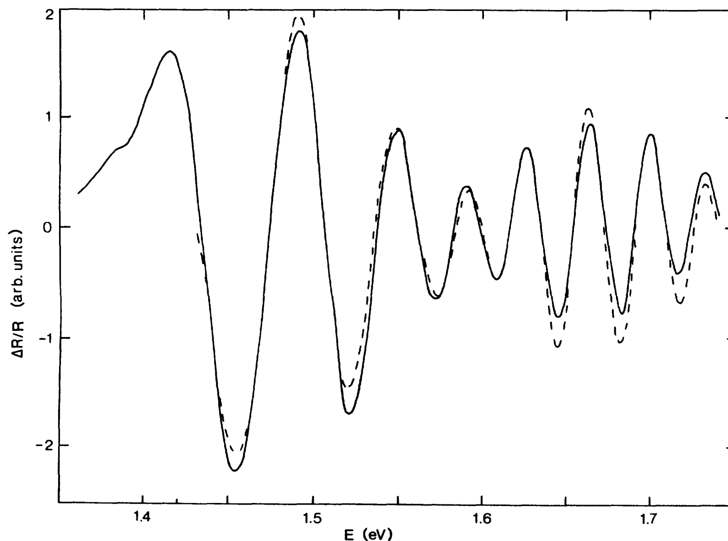

FIG. 4. Two-function fit to PR from the UN^+ sample in Fig. 2. The fit yields a 75-kV/cm field for the dark sample and a $V_s=0.12$ V at 0.2 mW/cm^2 intensity of 488-nm wavelength.

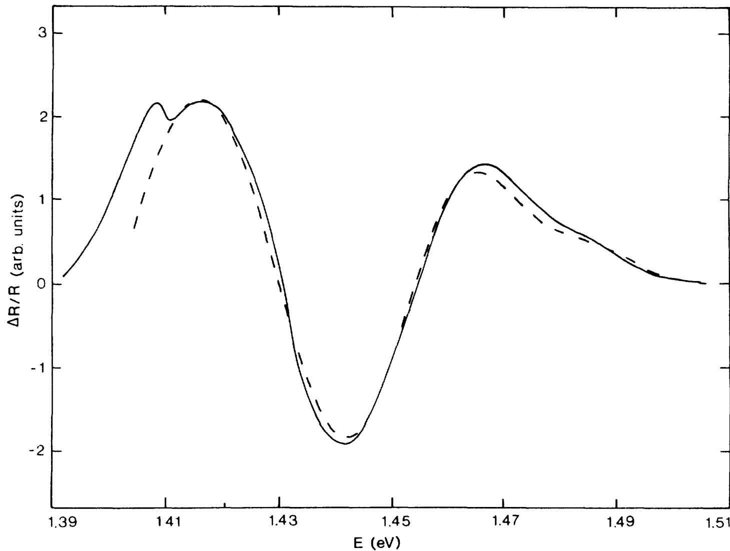

FIG. 5. Two-function fit to PR from the UP^+ sample. $\mathcal{E}_{\text{dark}}=65$ kV/cm and $V_s=0.32$ V at 0.2 mW/cm^2 intensity 488-nm wavelength.

UN^+ samples.

Figure 6 shows that V_b for UP^+ samples did not follow the same logarithmic behavior over a wide range of intensities. The logarithmic fit to V_b for UP^+ samples produced a $V_{b\,\max}$ of only 0.55 V. Furthermore, UP^+ PR was noisy and erratic below 5 μW/cm^2, whereas UN^+ and the plasma-treated samples gave well defined PR even at 2 μW/cm^2.

Both types of samples had identical histories, and have not shown appreciable change in PR over the past four years. The type of metal electrodes used in the discharge did not change the results appreciably; neither did the type of gas. The data presented here was for tungsten electrodes and H_2.

The effects of H_2 plasma discharge on surface contaminants[25,26] and the effects of vacuum and metal coating on V_s and V_F have been reported in Refs. 6, 11, 27, and 28. It is possible that metal deposition was responsible for the decrease in V_s from UP^+ samples upon plasma exposure. Plasma discharge left $\mathcal{E}_{\text{dark}}$ nearly the same in UP^+ and UN^+ samples. Plasma-treated samples had a well defined logarithmic behavior for V_b. By fitting Fig. 6 with logarithmic functions, we obtain $V_{b\max}=0.66$ V, and $V_{b\max}=0.76$ V for plasma-etched UP^+ and UN^+, respectively, in close agreement with the band-gap energy of 1.424 eV, and in close agreement with the calculated values of $\mathcal{E}_{\text{dark}}$.

To determine the origin of V_s we compared our results with Refs. 11 and 12. We fitted the results in Fig. 6 using the diode equations for (V_F-V_b) in terms of saturation current density J_s presented in Ref. 12 and J_0 presented in Ref. 11. For UN^+ and the plasma-treated samples we obtain $J_S\sim 65$ nA/cm^2 and 44 nA/cm^2, respectively. This compares very well with $J_S\sim 50$ nA/cm^2 listed in Ref. 12 for UN^+ and $(p\text{-}i\text{-}n)$ structures. On the other hand, untreated UP^+ sample gave a large $J_S=640$ nA/cm^2.

In comparing the results with Ref. 11, we obtain for

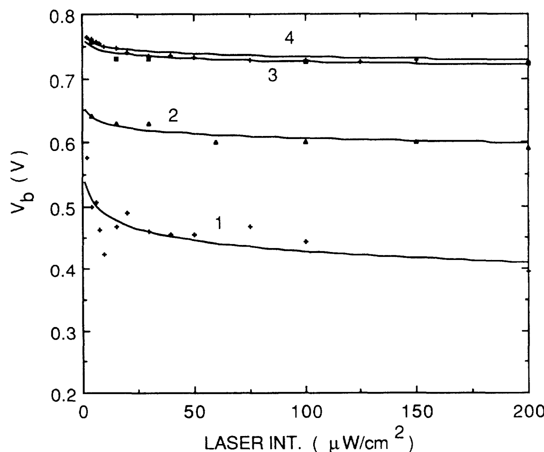

FIG. 6. Intensity dependence of FKO-determined V_b. Curve 1, UP^+ before plasma exposure. Curve 2, UP^+ three days after a 4-s plasma exposure. Curve 3, UN^+ sample. Curve 4, plasma-treated UN^+.

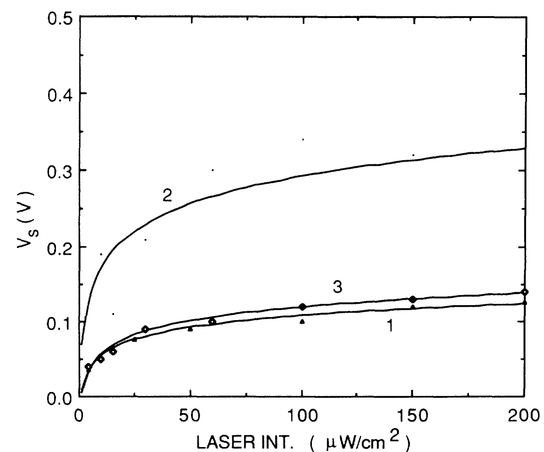

FIG. 7. Calculated values of V_s with logarithmic fit to $[(\mathcal{E}_{\text{dark}}-\mathcal{E}_{\text{illum}})\times 10^{-5}\text{ cm}]$ V. Curve 1, UN^+. Curve 2, UP^+. Curve 3, plasma-treated UP^+.

UN^+ and the plasma-treated samples $J_0 \sim 308$ and 365 nA/cm^2, respectively, which compares with $J_0 \sim 150$ nA/cm^2 obtained from the coefficients for UN^+ given in Refs. 6 and 11. Our UP^+ gave $J_0 \sim 830$ nA/cm^2, compared with $J_0 \sim 990$ nA/cm^2 obtained from UP^+ coefficients in Refs. 6 and 11.

Changes in saturation current with metal covering and changes in V_F with ultrahigh vacuum were reported in Refs. 11 and 28. Our minimum pressures were only in the mTorr range, and did not affect the samples prior to the plasma discharge.

Exposure to air on the order of days did not restore the PR from plasma-etched UP^+ samples. One UN^+ sample showed a decrease in $\mathcal{E}$ upon inadvertent and prolonged exposure to H_2 plasma at $\sim 10^{-3}$ Torr. That sample returned to normal when exposed to air, and was unaffected by a repeat of plasma exposure at $\sim 10^{-2}$ Torr.

SUMMARY

It appears that plasma-etched samples behave in accordance with a fixed V_F.[12] For prolonged discharge, metal deposition did occur but it did not appreciably affect the V_F of UN^+ samples, in agreement with the results that show that UN^+ has a firmly pinned V_F.[12] The FKO results in Fig. 6 indicate that plasma discharge could have changed V_F in UP^+ samples if we took the logarithmic fit of $V_{b\max}=0.55$ V at face value. However, the logarithmic fit for untreated UP^+ is poor with $R^2 \sim 0.6$, compared with the logarithmic fit to the untreated UN^+ and the plasma-etched UN^+ and UP^+ samples, where R^2 was above 0.92. Furthermore, $\mathcal{E}_{\rm dark}$ obtained from two functional fits for untreated UP^+ samples gave a V_F of 0.76 V, indicating that V_F was 0.76 V in dark UP^+ samples, but that V_F fluctuated with illumination. Thus, the decrease in V_s for UP^+ samples after plasma exposure could come from a firmed-up V_F that becomes insensitive to illumination, or from a factor-of-ten reduction of the saturation current J_s in UP^+ after H_2 and argon plasma treatment. The contribution from surface photomodulation effect to V_s for the UP^+ samples was ~ 0.2 V at 0.2 mW/cm^2 illumination. We believe that surface photomodulation comes from a fluctuation of V_F with trapping of photogenerated electrons at the free surface of UP^+ samples.

ACKNOWLEDGMENTS

Research was sponsored by the Air Force Office of Scientific Research/AFSC, United States Air Force, under Contract No. F49620-88-C-0053. We would like to thank our colleagues Neal Jahren for programming assistance, and Dr. Omar Manasreh (at ELRA), and Dr. W. C. Mitchel (at MLPO), of Wright Laboratory for cooperative research efforts under the USAF summer faculty research program.

---

*Present address: Physics Department, Cornell University, Ithaca, NY 14853.

[1] E. Y. Wang, W. A. Albers, and C. E. Bleil, in *Proceedings of the International Conference on II-VI Semiconductor Compounds, Providence, RI, 1967,* edited by D. G. Thomas (Benjamin, New York, 1968).

[2] O. J. Glembocki, B. V. Shanabrook, N. Bottka, W. T. Beard, and J. Comas, SPIE **524**, 86 (1985).

[3] D. E. Aspnes, Solid State Commun. **8**, 267 (1970); *Handbook on Semiconductors,* edited by M. Balkanski (North Holland, Amsterdam, 1980), Vol. 2, Chap. 4, p. 141.

[4] R. Glosser and N. Bottka, SPIE **794**, 88 (1987).

[5] M. H. Hecht, Phys. Rev. B **41**, 7918 (1990).

[6] X. Yin, H.-M. Chen, F. H. Pollak, Y. Chan, P. A. Montano, P. D. Kirchner, G. D. Pettit, and J. M. Woodall, Appl. Phys. Lett. **58**, 260 (1991).

[7] W. Zhou, C. H. Perry, L. Ma, K.-S. Lee, J. M. Worlock, A. Zrenner, F. Koch, and K. Ploog, J. Appl. Phys. **69**, 4075 (1991).

[8] W. E. Spicer, I. Lindau, P. Skeath, C. Y. Su, and Patrick Chye, Phys. Rev. Lett. **44**, 420 (1980).

[9] C. Van Hoof, K. Deneffe, J. De Boeck, D. J. Arent, and G. Borghs, Appl. Phys. Lett. **54**, 608 (1989).

[10] M. Sydor, J. R. Engholm, M. O. Manasreh, C. E. Stutz, L. Liou, and K. R. Evans, Appl. Phys. Lett. **56**, 1769 (1990).

[11] X. Yin, H.-M. Chen, F. H. Pollak, Y. Chan, P. A. Montano, P. D. Kirchner, G. D. Pettit, and J. M. Woodall, J. Vac. Sci. Technol. A **10**, 131 (1992).

[12] V. M. Airaksinen and H. K. Lipsanen, Appl. Phys. Lett. **60**, 2110 (1992).

[13] S. Chang, L. J. Brillson, Y. J. Kime, D. S. Rioux, P. D. Kirchner, G. D. Pettit, and J. M. Woodall, Phys. Rev. Lett. **64**, 2551 (1990).

[14] A. A. Bernussi, F. Ikawa, P. Motisuke, P. Basmaji, M. Siu Li, and O. Hipolito, J. Appl. Phys. **67**, 4149 (1990).

[15] H. Shen, M. Dutta, L. Fotiadis, P. G. Newman, R. P. Moerkirk, W. H. Chang, and R. N. Sacks, Appl. Phys. Lett. **57**, 2118 (1990).

[16] D. E. Aspnes, Phys. Rev. **147**, 554 (1966); **153**, 972 (1967); D. E. Aspnes, and A. A. Studna, Phys. Rev. B **7**, 4605 (1973); D. E. Aspnes, Phys. Rev. B **10**, 4228 (1974); D. E. Aspnes and A. Frova, Solid State Commun. **7**, 155 (1969).

[17] Joel Grover, Stephen Koeppen, and Paul Handler, Phys. Rev. B **4**, 2830 (1971).

[18] Shen Hongen, Ph.D. thesis, The City University of New York, 1987.

[19] P. R. Bevington, *Data Reduction and Error Analysis for the Physical Sciences* (McGraw-Hill, New York, 1969), pp. 235–240.

[20] R. N. Bhattacharya, H. Shen, P. Parayanthal, Fred H. Pollak, T. Coutts, and H. Aharoni, Phys. Rev. B **37**, 4044 (1988); Solar Cells **21**, 371 (1987).

[21] N. Bottka, D. K. Gaskill, R. S. Sillmon, R. Henry, and R. Glosser, J. Electron. Mater. **17**, 161 (1988).

[22] J. W. Garland, Z. Zhang, C. Kim, D. Yang, and P. M. Raccah, in *Photo-Induced Space Charge Effects in Semiconductors: Electro-Optics, Photoconductivity and the Photorefractive Effect,* MRS Symposia Proceedings No. 261, edited by D. D. Nolte, N. H. Haegel, and K. W. Goossen (Materials Research Society, Pittsburgh, 1992), p. 39.

[23] R. A. Batchelor and A. Hamnet, J. Appl. Phys. **71**, 2414 (1992).

[24]H. Shen and Fred H. Pollak, Phys. Rev. B **42**, 7097 (1990).
[25]M. Hong, R. S. Freund, K. D. Choquette, H. S. Luftman, J. P. Mannaerts, and R. C. Wetzel, Appl. Phys. Lett. **62**, 2658 (1993).
[26]C. Debiemme-Chouvy, D. Ballutaud, J. C. Pesant, and A. Etcheberry, Appl. Phys. Lett. **62**, 2254 (1993).
[27]D. K. Gaskill, N. Bottka, and R. S. Sillmon, J. Vac. Sci. Technol. B **6**, 1497 (1988).
[28]C. W. Wilmsen, P. D. Kirchner, and J. M. Woodall, J. Appl. Phys. **64**, 3287 (1988).